Retrograde inhibition by a specific subset of interpeduncular α5 nicotinic neurons regulates nicotine preference

Jessica L. Ables[a,b,c], Andreas Görlich[a,1], Beatriz Antolin-Fontes[a,2], Cuidong Wang[a], Sylvia M. Lipford[a], Michael H. Riad[a], Jing Ren[d,e,3], Fei Hu[d,e,4], Minmin Luo[d,e], Paul J. Kenny[c], Nathaniel Heintz[a,f,5], and Ines Ibañez-Tallon[a,5]

[a]Laboratory of Molecular Biology, The Rockefeller University, New York, NY 10065; [b]Department of Psychiatry, Icahn School of Medicine at Mount Sinai, New York, NY 10029; [c]Department of Neuroscience, Icahn School of Medicine at Mount Sinai, New York, NY 10029; [d]National Institute of Biological Sciences, Beijing 102206, China; [e]School of Life Sciences, Tsinghua University, Beijing 100084, China; and [f]Howard Hughes Medical Institute, The Rockefeller University, New York, NY 10065

Contributed by Nathaniel Heintz, October 23, 2017 (sent for review October 5, 2017; reviewed by Jean-Pierre Changeux and Lorna W. Role)

Repeated exposure to drugs of abuse can produce adaptive changes that lead to the establishment of dependence. It has been shown that allelic variation in the α5 nicotinic acetylcholine receptor (nAChR) gene *CHRNA5* is associated with higher risk of tobacco dependence. In the brain, α5-containing nAChRs are expressed at very high levels in the interpeduncular nucleus (IPN). Here we identified two nonoverlapping α5$^+$ cell populations (α5-^{Amigo1} and α5-^{Epyc}) in mouse IPN that respond differentially to nicotine. Chronic nicotine treatment altered the translational profile of more than 1,000 genes in α5-^{Amigo1} neurons, including neuronal nitric oxide synthase (*Nos1*) and somatostatin (*Sst*). In contrast, expression of few genes was altered in the α5-^{Epyc} population. We show that both nitric oxide and SST suppress optically evoked neurotransmitter release from the terminals of habenular (Hb) neurons in IPN. Moreover, in vivo silencing of neurotransmitter release from the α5-^{Amigo1} but not from the α5-^{Epyc} population eliminates nicotine reward, measured using place preference. This loss of nicotine reward was mimicked by shRNA-mediated knockdown of *Nos1* in the IPN. These findings reveal a proaddiction adaptive response to chronic nicotine in which nitric oxide and SST are released by a specific α5$^+$ neuronal population to provide retrograde inhibition of the Hb-IPN circuit and thereby enhance the motivational properties of nicotine.

nicotine | interpeduncular nucleus | retrograde | α5 nicotinic

The interpeduncular nucleus (IPN) is a single midline nucleus beneath the ventral tegmental area that receives the majority of its input from the medial habenula (MHb) and is reciprocally connected to the raphe nuclei (1–3). Recent evidence has highlighted a role of the IPN in nicotine consumption and withdrawal due to its high expression of the α5 nicotinic acetylcholine receptor (nAChR) subunit gene, the allelic variation in which is linked to increased risk of nicotine dependence (4–9).

The α5 subunit is considered an accessory component of functional nAChRs, active only when combined with both α- and β-nAChR subunits (8, 10). Incorporation of α5 to heteromeric nAChRs channels potently increases their sensitivity to nicotine (8). Mice with a null mutation of the *Chma5* gene self-administer more nicotine at higher, aversive doses, while reexpression of α5 in the MHb of α5 KO mice restored nicotine self-administration to wild-type (WT) levels, suggesting that α5 functions to limit nicotine intake (6). Viral-mediated expression of the most common genetic variant in *CHRNA5*, found in heavy smokers, α5D398N, in the MHb of β4-overexpressing (Tabac) mice, which otherwise show enhanced aversion to nicotine, was sufficient to increase their nicotine intake to WT levels (7). α5 is also expressed in cortical interneurons, and mice expressing the human α5D398N variant exhibit neurocognitive behavioral deficits that resemble the hypofrontality observed in patients with schizophrenia and addiction (9). α5 has also been implicated in nicotine withdrawal (11–13), characterized by somatic and affective symptoms, including increased anxiety (14, 15). Reexposure to nicotine during withdrawal increases intrinsic pacemaking activity of MHb cholinergic neurons (16). IPN neurons are activated during nicotine withdrawal, and optical activation of IPN GABAergic cells is sufficient to produce a withdrawal syndrome, while blockade of GABAergic cells in the IPN reduced symptoms of withdrawal (17). Taken together these studies highlight the critical role of α5 in regulating behavioral responses to nicotine.

Here we characterize two subpopulations of GABAergic neurons in the IPN that express α5: α5-^{Amigo1} and α5-^{Epyc} neurons. The translational profile of α5-^{Amigo1} cells, but not α5-^{Epyc}, shows enrichment for *Nos1* and *Sst*. While the presence of strong neuronal nitric oxide synthase (NOS1) expression in the IPN has been reported in cells that project to the dorsal raphe (DR) (18), no studies have been conducted to determine its function in IPN circuitry. Here, we show that the α5-^{Amigo1} population utilizes nitric oxide (NO) and somatostatin (SST) to provide retrograde inhibition of excitatory inputs from the MHb to the IPN. Consistent with this retrograde mechanism, MHb neurons are enriched with the receptors for NO (soluble guanylyl cyclases) and with SST receptors. We demonstrate that α5-^{Amigo1} neurons

Significance

The *CHRNA5-A3-B4* gene cluster, which encodes the α5, α3, and β4 nicotinic acetylcholine receptor subunits, has been genetically associated with high risk of developing nicotine dependence. Here we show that a specific α5 nicotinic receptor population in the midbrain interpeduncular nucleus (IPN) responds to chronic nicotine by increasing the expression of genes that regulate feedback inhibition of the medial habenula, the major source of input to the IPN. Inhibiting neurotransmitter release from this population of α5$^+$ neurons or reducing expression of one of these genes, *Nos1*, blocks the rewarding effects of nicotine. Our data identify molecular mechanisms that may explain the genetic link between *CHRNA5* and smoking predisposition in humans.

Author contributions: J.L.A., A.G., M.L., P.J.K., N.H., and I.I.-T. designed research; J.L.A., A.G., B.A.-F., C.W., S.M.L., M.H.R., J.R., and F.H. performed research; M.L., P.J.K., N.H., and I.I.-T. contributed new reagents/analytic tools; J.L.A., A.G., B.A.-F., M.H.R., J.R., F.H., M.L., N.H., and I.I.-T. analyzed data; and J.L.A., N.H., and I.I.-T. wrote the paper.

Reviewers: J.-P.C., CNRS, Institut Pasteur; and L.W.R., Stony Brook University.

The authors declare no conflict of interest.

[1]Present address: Life Sciences 2: Microbiology, Immunology, Neurosciences, Deutsche Forschungsgemeinschaft, 53170 Bonn, Germany.

[2]Present address: Clinical Sciences Centre, MRC London Institute of Medical Sciences, Hammersmith Hospital Campus, London, W12 0NN, United Kingdom.

[3]Present address: Department of Neurobiology, Stanford University, Stanford, CA 94305.

[4]Present address: Department of Cellular and Molecular Biology, Division of Neurobiology, University of California, Berkeley, CA 94720.

[5]To whom correspondence may be addressed. Email: heintz@rockefeller.edu or iibanez@rockefeller.edu.

This article contains supporting information online at www.pnas.org/lookup/suppl/doi:10.1073/pnas.1717506114/-/DCSupplemental.

increase their production of NO and SST in response to chronic nicotine, providing greater feedback inhibition onto MHb inputs. This action serves to limit the release of habenula-derived glutamate and enhances the motivational properties of nicotine. These results reveal a critical role for the α5-^{Amigo1} population of IPN cells in regulating the rewarding properties of nicotine through feedback inhibition of MHb inputs. Furthermore, our findings suggest that adaptive responses in this α5-^{Amigo1} controlled molecular circuitry likely plays an important role in regulating the development of nicotine dependence.

Results

α5-Expressing Neurons Can Be Subdivided into Two Populations. Using translating ribosomal affinity profiling (TRAP) (19) combined with RNA sequencing (RNA-Seq), we set out to determine which genes were being actively translated by discrete populations of α5^{+} cells in the IPN using *Chrna5*-Cre mice crossed to ribosome-tagged EGFP-L10a mice (Fig. 1*A*). In *Chrna5*-Cre mice, the *Chrna5-Chrna3-Chrnb4* gene cluster was overexpressed in IPN neurons (Fig. S1 and Datasets S1 and S2), which reduces the utility of these mice for investigating the behavioral actions of nicotine, since increased nAChR levels in MHb/IPN are known to affect nicotine reward and withdrawal processes (6, 7, 12, 20). Nevertheless, these mice provide a useful tool to target α5^{+} neurons and investigate their transcriptional mechanisms. Of the genes expressed in α5^{+} cells, we identified two highly enriched genes, *Amigo1* and *Epyc*, both encoding cell-surface adhesion proteins with relatively little-known function in the CNS. We characterized the translational profile of *Amigo1*-Cre::EGFP-L10a and *Epyc*-Cre::EGFP-L10a mice. We confirmed that both α5-^{Amigo1} (Fig. 1*B* and Dataset S3) and α5-^{Epyc} (Fig. 1*C* and Dataset S4) cells express the *Chrna5-Chrna3-Chrnb4* gene cluster at normal levels. Receptor and neurotransmitter expression profiling revealed that they are both GABAergic, as expected, and express a wide variety of acetylcholine (ACh), glutamate, GABA, and serotonin receptors. This profile is unique to the IPN and differs significantly from cholinergic MHb neurons (Fig. 1*D* and Datasets S1 and S3–S5). Consistent with existing data (17, 18), we found that α5^{+} cells were also enriched in *Sst* and *Nos1*; however, the α5-^{Amigo1} population was more highly enriched for these two transcripts than the α5-^{Epyc} population (Fig. 1*D*). MHb *ChAT* neurons express the receptors for both neurotransmitters at higher levels than IPN neurons (*Sstr2* and *Sstr4*, *Gucy1b3* and *Gucy1a3*) (Fig. 1*D*). High expression of these and other enriched TRAP-translated mRNAs in the two IPN populations matched the in situ hybridization signal of mRNA transcripts in the Allen Brain Atlas (Fig. S2). Analysis of the three populations revealed a great deal of similarity among them (Fig. 1*E*), although the profiles for α5-^{Amigo1} and α5-^{Epyc} indicate that these are distinct subpopulations of α5-expressing IPN neurons.

α5-^{Amigo1} and α5-^{Epyc} Cells Are Two Nonoverlapping Populations with Complementary Distribution in the IPN. To determine the distribution of the two subpopulations, we employed Cre-dependent adeno-associated virus (AAV)-DIO-EGFP-L10a to label nuclei, AAV-DIO-ChR2-eYFP to label axons and dendrites, and AAV-DIO-mCherry to label cell bodies and, to a lesser extent, dendrites (Fig. 2*A*). While both α5-^{Amigo1} and α5-^{Epyc} cells are distributed throughout the rostral nucleus of the IPN (IPR), α5-^{Epyc} cells are also found in the intermediate nucleus (IPI) (Fig. 2*A*). Note the complementary distribution of processes in the ventral half of the IPN between α5-^{Amigo1}- and α5-^{Epyc}-labeled neurons. To determine the overlap between populations, we crossed *Amigo1*-Cre mice with *Epyc*-EGFP mice and injected AAV-DIO-ChR2-mCherry to distinguish α5-^{Amigo1} cells (red) from α5-^{Epyc} cells (green) in the same animal (Fig. 2 *B–D* and Fig. S3). Confocal imaging in the IPN showed that no cells were colabeled and allowed us to trace the anterograde projections of each population (Fig. 2 *B* and *C* and Fig. S3 *A–C*). α5-^{Amigo1} cells contribute the majority of projections from the IPN to the median (MR), paramedian (PMR), and the DR, as well as the area surrounding the

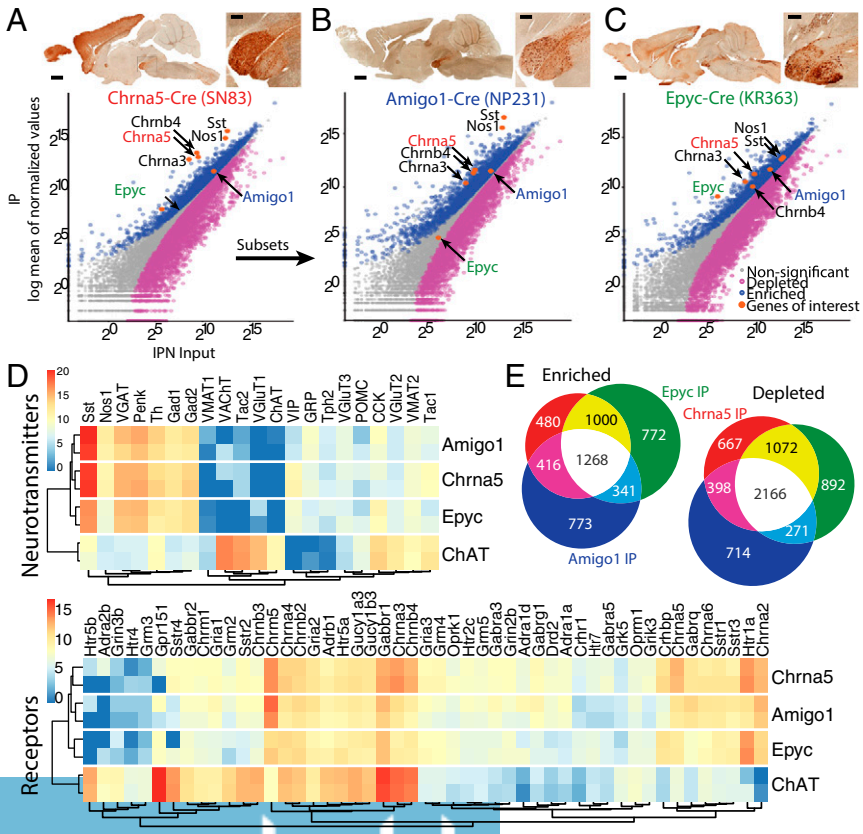

Fig. 1. TRAP profiling reveals two subsets of α5 neuronal populations in the IPN. (*A*) *Chrna5*-Cre mice (*Top*) crossed to EGFP-L10a reporter mice were used for TRAP. (*Bottom*) Scatterplots of average TRAP IP samples (*y* axis) versus input samples (*x* axis) represent enriched (>0.6 $\log_2$ fold change, blue) or depleted (less than −0.6 $\log_2$ fold change, magenta) translated mRNAs. Highly enriched mRNAs for *Amigo1* and *Epyc* were identified for further characterization. (*B*) *Amigo1*-Cre::EGFP-L10a mice (*C*) and *Epyc*-Cre::EGFP-L10a mice were employed for TRAP and showed enriched mRNAs for *Chrna5-Chrna3-Chrnb4* as indicated in the corresponding scatterplots. (*A–C*) (Scale bar: low magnification 1 mm, high magnification 200 μm.) Images courtesy of GENSAT.org. (*D*) Expression levels (z-score transformed normalized counts) of receptors and neurotransmitters in the three IPN populations as well as in *ChAT* MHb neurons. (*E*) α5-^{Amigo1} and α5-^{Epyc} cells share a large number of enriched and depleted mRNAs with *Chrna5* cells.

laterodorsal tegmentum (LDTg). There is also a small ascending projection back to the MHb and to the thalamus (Fig. S3*A*). Note that the *Epyc*-EGFP population appears to be composed of several local populations in the IPN and along the IPN–raphe axis (Fig. 2 *B* and *C* and Fig. S3*C*). Within the IPN, local projections between the two IPI areas were evident (Fig. 2*A* and Fig. S3*C*) and confirmed by streptavidin filling in acute slices (Fig. S3*E*). We next performed retrograde experiments to trace the monosynaptic inputs to α5-^{Amigo1} and α5-^{Epyc} populations using Cre-dependent rabies virus (21). We found that both α5-^{Amigo1} and α5-^{Epyc} populations receive major input from the MHb and raphe (Fig. 2 *E* and *F* and Fig. S3 *D–F*). Smaller sources of direct input to the IPN included the septum and a previously uncharacterized projection from the prefrontal cortex. No striking differences were observed between α5-^{Amigo1} and α5-^{Epyc} inputs, although α5-^{Amigo1} appeared to have a larger component of input from the medial septum and dorsal raphe. Together these data show that α5-^{Amigo1} and α5-^{Epyc} are two nonoverlapping IPN populations that both receive their main input from the MHb, but that one projects locally (α5-^{Epyc}) while the other (α5-^{Amigo1}) sends long projections to raphe and LDTg areas.

Chronic Nicotine Increases *Sst* and *Nos1* in α5-^{Amigo1} Neurons. Given that habenulo-interpeduncular α5 has a critical role in nicotine reward and withdrawal (6, 7, 11), we sought to determine whether nicotine can induce molecular changes in IPN neurons carrying α5 receptors. To this end, we administered nicotine in the drinking water of *Amigo1*-Cre::EGFP-L10a and *Epyc*-Cre::EGFP-L10a mice for 6 wk before performing TRAP. We found that chronic nicotine significantly changed the translational levels of a large number of genes in α5-^{Amigo1} cells (300 mRNAs up-regulated and 1,539 mRNAs down-regulated, Datasets S6–S9). Strikingly, despite the fact that α5-^{Epyc} cells express similar amounts of *Chrna5*-translated mRNAs as α5-^{Amigo1} (Fig. 3*A*), chronic nicotine altered the levels of a much smaller set of genes in these cells (24 mRNAs up-regulated and 51 down-regulated mRNAs, Datasets S10 and S11). The RNA-Seq normalized counts for the different nicotinic receptor subunits did not change with chronic nicotine in any of the populations, except for a significant increase of *Chrna2* mRNAs in α5-^{Amigo1} cells (Fig. 3*A* and Datasets S6–S14). Of the large number of mRNAs regulated in α5-^{Amigo1} cells, *Sst* and *Nos1* mRNA induction was remarkable ($\log_2$ fold change 1.37 for *Nos1* 3′ UTR and 2.67 for *Sst*, Fig. 3*B* and Datasets S6–S9). We confirmed that this increase in translated mRNAs corresponded to an increase at the protein level (Fig. 3 *C* and *D*). Comparison of TRAP mRNA-Seq of different brain cell types showed that *Nos1*- and *Sst*-translated mRNA levels are extremely high in α5-^{Amigo1} cells, while subunits for the NO receptor soluble guanylyl cyclase (GC) *Gucy1a3*, *Gucy1b3*, and SST receptors *Sstr2* and *Sstr4* are expressed in several cell types and at high levels in cholinergic habenular neurons (22, 23) (Fig. 3*E*). Expression of NOS1 in *Amigo1*-Cre but not *Epyc*-Cre neurons, as well as GUCY1B3 and SSTR2 in the MHb and its projections to the IPN were confirmed by immunohistochemistry (IHC) (Fig. 3*F* and Fig. S4). These data demonstrate that chronic exposure to nicotine strongly and specifically impacts the α5-^{Amigo1} subpopulation of IPN neurons, suggesting adaptive changes in these cells that may play a crucial role in the establishment of dependence.

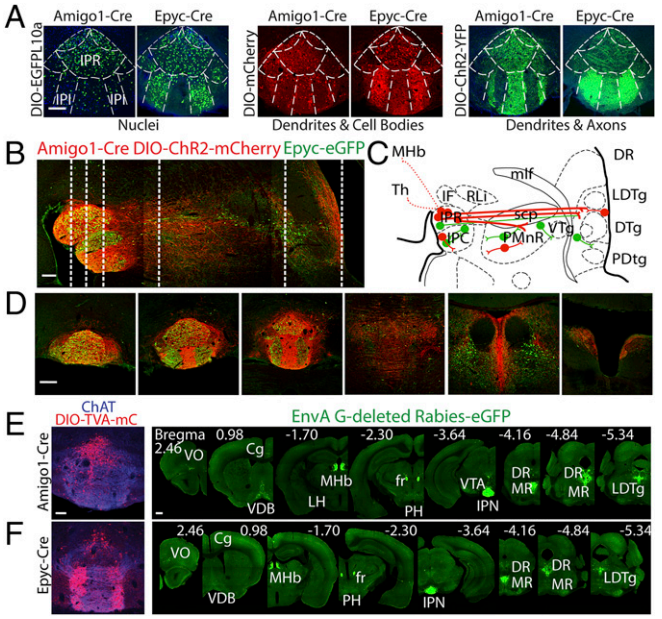

Fig. 2. α5-^{Amigo1} and α5-^{Epyc} cells are two distinct, complementary IPN populations. (*A*) *Amigo1*-Cre and *Epyc*-Cre mice were injected with the indicated AAVs to label distinct cell compartments and determine the population distribution. α5-^{Amigo1} and α5-^{Epyc} cells are present in the rostral subnucleus (IPR), but α5-^{Amigo1} cells are largely excluded from the intermediate subnuclei (IPI), where α5-^{Epyc} cells are densely distributed. (Scale bar: 100 μm.) (*B*) Anterograde tracing in *Epyc*-EGFP × *Amigo1*-Cre mice injected with DIO-ChR2-mCherry shows dense *Amigo1* projections (red) from IPN to caudal structures relative to *Epyc* projections (green). (Scale bar: 200 μm.) (*C*) Schematic representation of Amigo projections (red) and *Epyc* projections (green). *Epyc* cells appear to be a series of local interneurons along the IPN–raphe axis, with a relatively minor projection from IPN to raphe and caudal structures. (*D*) Coronal sections corresponding to the dashed lines in *A*. (Scale bar: 200 μm.) (*E* and *F*) Retrograde tracing with rabies virus in *Amigo1*-Cre and *Epyc*-Cre mice. Coronal sections of IPN from *Amigo1*-Cre (*E*) or *Epyc*-Cre (*F*) mouse injected with DIO-TVA-mCherry and DIO-rabies G protein (1:1, red, *Left*) followed by injection of EnvA G-deleted rabies-EGFP to label monosynaptic inputs (green, *Right*). (Scale bar: low magnification 500 μm, high magnification 100 μm.)

IPN Neurons Provide Feedback Inhibition to MHb via NO and SST. Given that IPN α5-^{Amigo1} neurons enriched in *Nos1* and *Sst* are synaptically connected to MHb neurons (Fig. 2), and that MHb *ChAT* neurons express the receptors for NO and SST (Figs. 1 and 3), we sought to determine whether there was a functional connection between the IPN and MHb utilizing these neurotransmitters. We performed slice electrophysiology in *ChAT*-ChR2 mice. These mice express channelrhodopsin in cholinergic MHb neurons, which heavily innervate the NOS1-enriched area in the IPN (Fig. 4 *A–C*). Photostimulation of cholinergic axon terminals has been shown to evoke postsynaptic responses in IPN neurons mediated by glutamate and ACh corelease (24). Application of sodium nitroprusside (SNP), a nitric oxide donor, in the presence of nAChR blockers, suppressed light-evoked excitatory postsynaptic currents (EPSCs) in the IPN, indicating that NO decreases glutamate release from MHb terminals (Fig. 4 *D–F*). This effect was long lasting and recovered minimally after washout. Glutamate release from MHb terminals was also suppressed by erythro-9-(2-hydroxy-3-nonyl)adenine (EHNA), an inhibitor of the cGMP-activated phosphodiesterase PDE2A, and was not further suppressed by addition of SNP (Fig. S5), indicating that the NO suppression is mediated by an increase in cGMP in habenular neurons. Similarly, application of SST to *ChAT*-ChR2 brain slices reduced light-evoked EPSCs in the IPN, with greater recovery after washout (Fig. 4 *G–I*). This presynaptic inhibition is most likely mediated by SSTR2 and SSTR4 receptors ($G_{i/o}$ signaling), which are heavily expressed in MHb *ChAT* neurons (Figs. 1 and 3). These results demonstrate strong presynaptic inhibition of habenular neurons by NO and SST. Since nicotine up-regulates *Nos1* and *Sst* expression in α5-^{Amigo1} cells, these data suggest important physiological and behavioral roles for these neurotransmitters in modulation of synaptic transmission by cAMP- and cGMP-signaling pathways in the MHb/IPN circuit.

Silencing α5-^{Amigo1} Cells or Inhibiting NO Production in the IPN Eliminates Nicotine Preference. Finally, to investigate the functional role that α5 cells might play in the behavioral response to nicotine, we utilized AAVs expressing Cre-dependent membrane-tethered Ca^{2+}-channel toxins (tToxins) that prevent neurotransmitter release (25) to silence either α5-^{Amigo1} or α5-^{Epyc} cells in the IPN (Fig. 5*A*). Mice were subjected to a battery of tests to explore any behavioral consequence

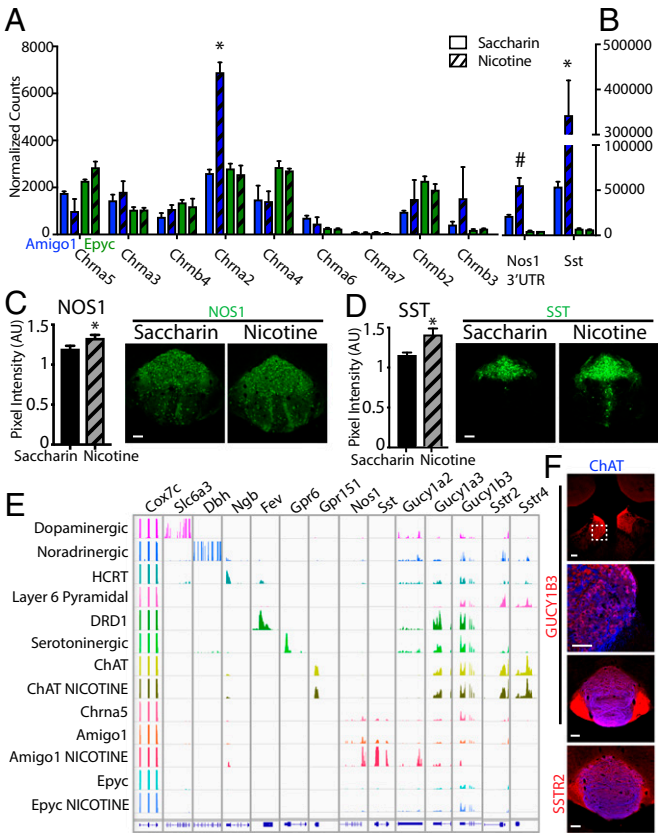

Fig. 3. Chronic nicotine up-regulates SST and NOS1 in α5-^{Amigo1} cells. (*A*) Normalized RNA-Seq counts of nAChRs in *Amigo1*-Cre::EGFP-L10a (blue) and *Epyc*-Cre::EGFP-L10a (green) mice after 6 wk of saccharin (solid bars) or nicotine (striped bars). Note that only *Chrna2* is up-regulated in α5-^{Amigo1} cells. (*B*) Normalized RNA-Seq counts of *Nos1* 3′ UTR and *Sst* in *Amigo1* and *Epyc* mice after 6 wk of nicotine (*$P_{adj} < 0.05$, #$P_{adj} = 0.08$, DESeq2). (*C*) Quantification of IHC pixel intensity in the IPN confirms increased expression of NOS1 (*C*) and SST (*D*) after chronic nicotine (*$P < 0.05$, unpaired two-tailed *t* test). (Scale bar: 100 μm.) (*E*) Integrated Genomics Viewer (IGV 2.3) of cell-specific translated mRNAs. *Top* row indicates *Cox7c*, a housekeeping gene, followed by positive control genes expressed in each cell type, followed by *Nos1* and *Sst* and their respective receptors *Gucy1a2*, *Gucy1a3*, *Gucy1b3*, *Sstr2*, and *Sstr4*. Note the specific increase in expression of *Nos1* and *Sst* in *Amigo1* mice after 6 wk of nicotine treatment. (*F*) GUCY1B3 is expressed in the cell bodies and terminals of cholinergic MHb cells, and SSTR2 in MHb terminals in the IPN. (Scale bar: low magnification 100 μm, high magnification 50 μm.)

of silencing α5 cells. No significant differences were observed between control- and tToxin-injected animals in locomotion, anxiety, despair, or in sensory gating tests (Dataset S15). We performed conditioned place preference (CPP) for a rewarding dose of nicotine, 0.35 mg/kg free base. Silencing α5-^{Amigo1} cells prevented place preference for nicotine, whereas silencing α5-^{Epyc} cells had no effect (Fig. 5*B*). Similar to CPP results, *Amigo1*-Cre mice injected with tToxins consumed less nicotine than control mice, while silencing IPN cells in *Epyc*-Cre mice had no effect on consumption (Fig. 5*C*). Given these differences in the response of nicotine between populations, we performed electrophysiological recordings. Patch-clamp recordings with local puff application of nicotine showed large nAChR-evoked currents in α5-^{Amigo1} cells (Fig. 5*D*). Within the α5-^{Epyc} population we distinguished two types of populations with distinct morphology and basic electrophysiological properties (Fig. 5*E* and Fig. S6). α5-^{Epyc} cells in the IPR showed similar nicotine-evoked current amplitudes as α5-^{Amigo1} cells (the majority of which are in the IPR), while strikingly, α5-^{Epyc} cells in the IPI, which constitute the majority of the α5-^{Epyc} population, responded poorly to nicotine (Fig. 5*E*). Given these IPN regional differences in the response to nicotine and the enrichment of NOS1 in the IPR, we next sought to determine a possible role of *Nos1* in nicotine reward. We injected WT mice with AAV-expressing shRNA against *Nos1* (Fig. 5*F*) and found that, similar to silencing α5-^{Amigo1} cells, knockdown of *Nos1* locally in the IPN was sufficient to block preference for a rewarding dose of nicotine (Fig. 5*G*). These results demonstrate that a specific subset of α5^{+} IPN neurons respond at the molecular level to chronic nicotine exposure and that these adaptive changes may in turn play a crucial role in the establishment of dependence.

Discussion

In this study, we employed translational profiling to identify a neuronal population in the IPN that expresses high levels of α5 nAChRs and responds to chronic nicotine by up-regulating *Nos1* and *Sst*. We find that NO and SST application in the IPN abolishes synaptic release from habenular neurons enriched in receptors for both neurotransmitters. Inhibition of retrograde signaling, either by silencing neurotransmitter release from the α5-^{Amigo1} population or knocking down NO production in the IPN, eliminates preference for a rewarding dose of nicotine. Our data demonstrate a strong effect of nicotine on the production of NO and SST and delineate a signaling pathway that provides presynaptic inhibition as an adaptive mechanism to locally reduce the activity of the Hb-IPN circuit in response to chronic nicotine.

Unlike classical neurotransmitters that transfer information from axonal presynaptic release sites to postsynaptic receptors, neuropeptides and NO ignore directionality of information flow and can transmit signals outside the typical synapse. Neuropeptides, including SST, can be released from dendrites, soma, and axons (26), while NO is a membrane-permeable hydrophobic gas (27, 28). While this is a study that examines the functional role of SST and NO in the IPN, critical roles for NO and SST signaling in neuronal plasticity and transmission have been established in other areas of the brain (29–31). For example, SST interneurons

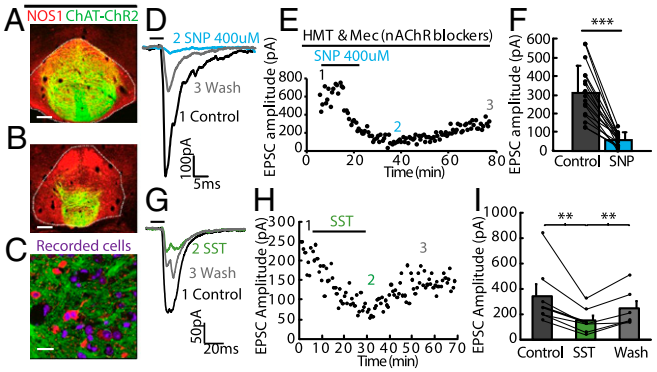

Fig. 4. NO and SST inhibit evoked neurotransmitter release from axonal terminals of MHb neurons to the IPN. (*A* and *B*) Coronal sections from a *ChAT*-ChR2-EYFP mouse showing expression of NOS1 (red) in ChR2-EYFP^{+} terminals (green) in the IPN. (Scale bar: 100 μm.) (*C*) High-magnification view shows that ChR2-EYFP–labeled axonal terminals (green) encircle NOS1 immunopositive neurons (red) in the IPN. (Scale bar: 20 μm.) (*D* and *E*) Representative electrophysiological traces (*D*) and plot of EPSC amplitude versus time (*E*) show that application of the NO donor sodium nitroprusside (SNP) (400 μM) into the bath solution completely abolishes fast EPSCs evoked by brief blue light illumination (5 ms; horizontal bar) in the presence of nAChR blockers hexamethonium (HMT) and mecamylamine (Mec) and this blockade lasted for over 1 h. (*F*) Summary data show that SNP eliminates EPSCs (***$P < 0.001$, paired *t* test, $n = 15$ cells). Separate lines represent data from individual neurons. Control indicates EPSCs measured in nAChRs blockers. (*G–I*) Representative electrophysiological traces (*G*) and plot of EPSC amplitude versus time (*H*) show that application of SST (1 μM) reduces fast EPSCs evoked by brief blue light illumination (5 ms; horizontal bar) and this inhibition lasted for over 20 min in wash solution. (*I*) Summary data show that SST reduces EPSCs (**$P < 0.005$, paired *t* test, $n = 6$ cells). Separate lines represent data from individual neurons. Error bars indicate SEM.

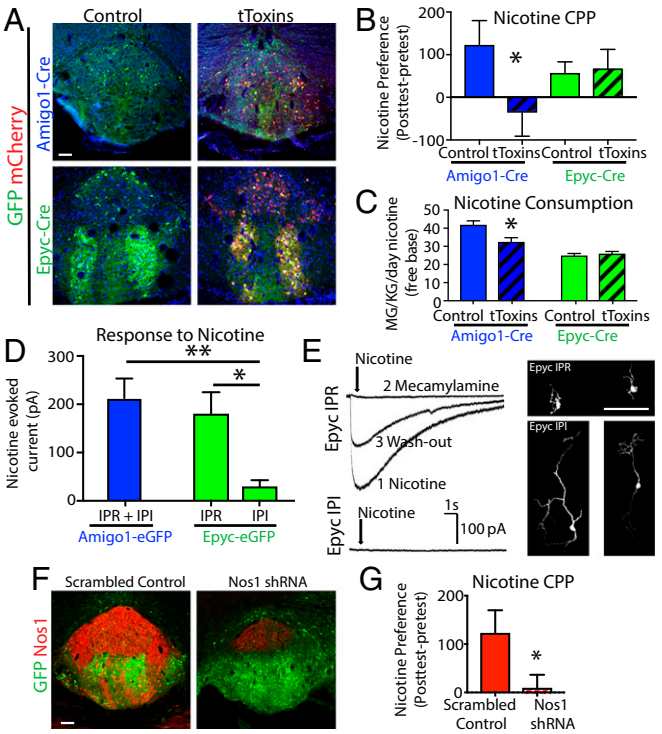

Fig. 5. Blocking neurotransmission of α5-^{Amigo1} cells or knocking down *Nos1* in IPN prevents nicotine preference. (*A*) Viral expression in control and tToxin-injected mice. (Scale bar: 100 μm.) (*B*) Place preference for a rewarding dose of nicotine (0.35 mg/kg, free base, i.p.) was eliminated in *Amigo1*-Cre mice expressing tToxins but not *Epyc*-Cre mice (*$P < 0.05$, unpaired one-tailed *t* test). (*C*) Average daily nicotine consumption was reduced in *Amigo1*-Cre but not *Epyc*-Cre mice injected with tToxins compared with control (*$P < 0.05$, unpaired two-tailed *t* test). (*D*) Average current amplitude of nicotine-evoked responses in *Amigo1* and *Epyc* cells located in IPR and IPI regions (*$P < 0.05$, **$P < 0.01$, unpaired two-tailed *t* test, $n = 11$, 7, 8 cells, respectively). (*E*) Representative nicotine currents in IPR and IPI *Epyc* neurons and photomicrographs of streptavidin-filled neurons. (Scale bar: 100 μm.) (*F*) NOS1 expression is reduced by >75% in WT animals injected with *Nos1* shRNA but not with a scrambled control virus. (Scale bar: 100 μm.) (*G*) Knockdown of *Nos1* in the IPN of WT mice blocked place preference for nicotine (0.35 mg/kg, free base, i.p., *$P < 0.05$, unpaired one-tailed *t* test).

in the neocortex serve as prominent sources of inhibition, in part via activation of SSTR2/4 ($G_{i/o}$ inhibitory) that reduce cAMP and suppress neuronal firing in pyramidal neurons (29). We believe a similar situation occurs in the MHb/IPN where SST release from IPN activates habenular SSTR2/4, reduces cAMP, and inhibits presynaptic neurotransmission. In favor of this hypothesis, raising cAMP levels has been shown to increase glutamatergic EPSC amplitudes in the IPN (32), and activation of GLP-1 receptors (G_s coupled) diminished nicotine self-administration, an effect that can be counteracted by a cAMP inhibitor (33). Likewise, in habenular neurons cGMP production has been shown to activate PDEA2, which depletes cAMP levels and suppresses presynaptic neurotransmission (34). We predict that NO binding to soluble GC activates this cascade, since NO suppression of glutamate release is blocked by PDE2A inhibitors. Taken together these and the present studies indicate that cGMP–cAMP fluctuations in habenular terminals critically influence nicotine consumption.

The MHb/IPN circuit is structurally complex, with multiple en passant synapses present on MHb axons that crisscross the IPN multiple times (35) (Fig. S3*D*). This unique anatomy may be required to facilitate retrograde volume transmission of NO and possibly SST. It has been shown, for example, that an array of puncta 2 μm apart is necessary for volume transmission by NO (36). Although glutamate release from the MHb may be sufficient to activate NOS1, as canonically its activation is directly linked to calcium influx through NMDA receptors, NOS1 can also be coupled to nicotinic receptors as previously observed in autonomic neurons in the periphery (37). We speculate that the high-frequency corelease of glutamate and ACh by MHb is required for maximal NO production. Data from cortex and hippocampus suggest that spike burst patterns are highly effective at inducing neuropeptide and NO release, with increased frequency of action potentials increasing neuropeptide release from both axons and dendrites (26, 36). Given that habenular neurons employ pacemaking, firing at roughly 10–20 Hz (16), one could postulate that the increase in SST seen with chronic nicotine is due to increased pacemaking of habenular neurons. The mechanism of neuropeptide release, like neurotransmitter release, is calcium dependent, and our findings here suggest that tToxins likely affect release of SST by blocking calcium influx associated with depolarization, as it has been shown that some neuropeptides utilize P/Q- and N-type voltage-gated calcium channels for dendritic release (26).

One of the most striking findings is that despite expressing similar amounts of α5 receptors, the α5-^{Epyc} population demonstrated no appreciable molecular or behavioral changes in response to acute or chronic nicotine. Is there a limiting factor? A possible explanation is that the α2 nicotinic receptor subunit is strongly upregulated with nicotine in α5-^{Amigo1} cells (Fig. 3*A*). α2 predominantly associates with β2 subunits in the IPN (38) and reconstitution of α2α5β2 heterodimers in lipid bilayers forms functional channels with nanomolar agonist affinity similar to α4β2 receptors (39). Since α5, α2, and β2 subunits are well expressed in the IPN (Fig. 3), and α5 and α2 null mice have similar nicotine-related phenotypes: potentiated self-administration (6, 40) and reduced withdrawal in a habituated environment (11), it seems likely, therefore, that these subunits work together in the IPN and that nicotine stimulation of α2 further amplifies the response of α5-^{Amigo1} cells to nicotine. In favor of this hypothesis we observed high nicotine-evoked currents in the IPR where α2 and α5 coexist [see in situ hybridization (ISH) in Fig. S2] but not in the IPI region where the nonresponsive α5-^{Epyc} subpopulation is located (Fig. 5). Interestingly human genetic studies have linked nicotine dependence not only to *CHRNA5* variants (4, 41) but also more recently to *CHRNA2* (42). IPI α5-^{Epyc} cells also specifically express *Lynx1* (Fig. S2 and Dataset S4), a prototoxin modulator that limits nAChR currents, that could have an important influence on its responses to nicotine (43). The fact that *ChAT* MHb neurons also display no translational changes to nicotine exposure (Fig. 3 and Datasets S13 and S14) provides additional support for the hypothesis that responses to chronic nicotine must reflect specific nAChRs and modulators that are characteristic of that cell type.

Although the molecular adaptations that occur in α5-^{Amigo1} neurons must play an important role in the behavioral differences we have documented here, it is important to note that their signaling to the raphe and LDTg (Fig. 2 and Fig. S3) may also modulate the circuit. In this context, it is particularly interesting that serotonergic neurons in the raphe also express high amounts of the soluble GC dimer *Gucy1a3/b3* (Fig. 3, serotoninergic cells). Since the IPN is reciprocally connected to raphe and retrogradely connected to MHb, nicotine activation of the IPN could release NO to synchronously suppress the activity of MHb, IPN, and raphe. This possibility will require additional investigation of the specific responses of raphe neurons to α5-^{Amigo1} activation in the context of NO inhibition. Taken together, these results highlight the critical role of a unique α5 population in the IPN in detecting and signaling nicotine in the brain.

Methods

Details for all materials and methods can be found in *SI Materials and Methods*.

Mice. All studies were done in accordance with National Institutes of Health and Institutional Animal Care and Use guidelines. All procedures and protocols were approved by the Animal Care Committee of The Rockefeller University. Information regarding specific lines used are in *SI Materials and Methods*.

Translating Ribosome Affinity Purification and RNA-Seq. TRAP was conducted in at least duplicates as previously described (*SI Materials and Methods*). Immunoprecipitated (IP) and total mRNA fractions purified for TRAP were subjected to RNA sequencing on an Illumina HiSEq 2500.

Histology and Confocal Imaging. Staining of sections from *Chrna5*-eGFP, *Amigo1*-Cre, and *Epyc*-Cre mice with anti-GFP, anti-mCherry, anti-*ChAT*, anti-NOS1, anti-GUCY1B3, and anti-SSTR2 antibodies was done as described in *SI Materials and Methods*.

Nicotine Treatment. All nicotine doses are reported as free base. For acute nicotine, mice were administered 0.35 mg/kg, i.p. For chronic nicotine exposure, mice were given nicotine (500 mg/L) in the drinking water for 6 wk.

Surgical Procedures for Microinjections. Mice were injected with the indicated virus into the IPN (coordinates, anteroposterior, –3.6 mm from Bregma; mediolateral, –1.7 mm from midline; dorsoventral, –5 mm from dura, 20° angle).

Electrophysiological Recordings. For whole-cell recordings of the NO and SST effects, patch pipettes were filled with internal solution that contained the following (in millimoles): 130 K-gluconate, 10 Hepes, 0.6 EGTA, 5 KCl, 3 Na_2ATP, 0.3 Na_3GTP, 4 $MgCl_2$, and 10 Na_2-phosphocreatine. Cells were recorded at 30–33 °C. For full details see *SI Materials and Methods*.

Statistical Analysis. Sets of data are presented by their mean values and SEMs. The unpaired one- or two-tailed Student *t* test was used when comparing two sets of data with normal distribution.

ACKNOWLEDGMENTS. We thank Awni Mousa for analysis of TRAP data; Marian Mellen for critical discussion of the manuscript and the data; and Laura Kus, Syed Samin Shehab, Claire Warriner, and Johana Alvarez for assistance. A.G. received Deutsche Forschungsgemeinschaft Fellowship GO 2334/1-1. This work was supported by NIH P30 DA035756-01 (to N.H. and I.I.-T.), DA020686 (to P.J.K.), National Natural Science Foundation of China Grants 91432114 and 91632302 (to M.L.), and the Leon Black Family Foundation (I.I.-T. and N.H.). N.H. is a Howard Hughes Medical Institute investigator.

1. Klemm WR (2004) Habenular and interpeduncularis nuclei: Shared components in multiple-function networks. *Med Sci Monit* 10:RA261–RA273.
2. Boulos LJ, Darcq E, Kieffer BL (2017) Translating the habenula: From rodents to humans. *Biol Psychiatry* 81:296–305.
3. Antolin-Fontes B, Ables JL, Gorlich A, Ibanez-Tallon I (2015) The habenulo-interpeduncular pathway in nicotine aversion and withdrawal. *Neuropharmacology* 96: 213–222.
4. Bierut LJ, et al. (2008) Variants in nicotinic receptors and risk for nicotine dependence. *Am J Psychiatry* 165:1163–1171.
5. Thorgeirsson TE, et al. (2008) A variant associated with nicotine dependence, lung cancer and peripheral arterial disease. *Nature* 452:638–642.
6. Fowler CD, Lu Q, Johnson PM, Marks MJ, Kenny PJ (2011) Habenular α5 nicotinic receptor subunit signalling controls nicotine intake. *Nature* 471:597–601.
7. Frahm S, et al. (2011) Aversion to nicotine is regulated by the balanced activity of β4 and α5 nicotinic receptor subunits in the medial habenula. *Neuron* 70:522–535.
8. Ramirez-Latorre J, et al. (1996) Functional contributions of alpha5 subunit to neuronal acetylcholine receptor channels. *Nature* 380:347–351.
9. Koukouli F, et al. (2017) Nicotine reverses hypofrontality in animal models of addiction and schizophrenia. *Nat Med* 23:347–354.
10. Taly A, Corringer PJ, Guedin D, Lestage P, Changeux JP (2009) Nicotinic receptors: Allosteric transitions and therapeutic targets in the nervous system. *Nat Rev Drug Discov* 8:733–750.
11. Salas R, Sturm R, Boulter J, De Biasi M (2009) Nicotinic receptors in the habenulo-interpeduncular system are necessary for nicotine withdrawal in mice. *J Neurosci* 29: 3014–3018.
12. Pang X, et al. (2016) Habenula cholinergic neurons regulate anxiety during nicotine withdrawal via nicotinic acetylcholine receptors. *Neuropharmacology* 107:294–304.
13. Jackson KJ, Martin BR, Changeux JP, Damaj MI (2008) Differential role of nicotinic acetylcholine receptor subunits in physical and affective nicotine withdrawal signs. *J Pharmacol Exp Ther* 325:302–312.
14. Jonkman S, Henry B, Semenova S, Markou A (2005) Mild anxiogenic effects of nicotine withdrawal in mice. *Eur J Pharmacol* 516:40–45.
15. Isola R, Vogelsberg V, Wemlinger TA, Neff NH, Hadjiconstantinou M (1999) Nicotine abstinence in the mouse. *Brain Res* 850:189–196.
16. Görlich A, et al. (2013) Reexposure to nicotine during withdrawal increases the pacemaking activity of cholinergic habenular neurons. *Proc Natl Acad Sci USA* 110: 17077–17082.
17. Zhao-Shea R, Liu L, Pang X, Gardner PD, Tapper AR (2013) Activation of GABAergic neurons in the interpeduncular nucleus triggers physical nicotine withdrawal symptoms. *Curr Biol* 23:2327–2335.
18. Quina LA, Harris J, Zeng H, Turner EE (2017) Specific connections of the interpeduncular subnuclei reveal distinct components of the habenulopeduncular pathway. *J Comp Neurol* 525:2632–2656.
19. Heiman M, Kulicke R, Fenster RJ, Greengard P, Heintz N (2014) Cell type-specific mRNA purification by translating ribosome affinity purification (TRAP). *Nat Protoc* 9: 1282–1291.
20. Slimak MA, et al. (2014) Habenular expression of rare missense variants of the β4 nicotinic receptor subunit alters nicotine consumption. *Front Hum Neurosci* 8:12.
21. Wall NR, Wickersham IR, Cetin A, De La Parra M, Callaway EM (2010) Monosynaptic circuit tracing in vivo through Cre-dependent targeting and complementation of modified rabies virus. *Proc Natl Acad Sci USA* 107:21848–21853.
22. Thorvaldsdóttir H, Robinson JT, Mesirov JP (2013) Integrative Genomics Viewer (IGV): High-performance genomics data visualization and exploration. *Brief Bioinform* 14: 178–192.
23. Robinson JT, et al. (2011) Integrative genomics viewer. *Nat Biotechnol* 29:24–26.
24. Ren J, et al. (2011) Habenula "cholinergic" neurons co-release glutamate and acetylcholine and activate postsynaptic neurons via distinct transmission modes. *Neuron* 69:445–452.
25. Auer S, et al. (2010) Silencing neurotransmission with membrane-tethered toxins. *Nat Methods* 7:229–236.
26. van den Pol AN (2012) Neuropeptide transmission in brain circuits. *Neuron* 76:98–115.
27. Nedeianu S, Páli T, Marsh D (2004) Membrane penetration of nitric oxide and its donor S-nitroso-N-acetylpenicillamine: A spin-label electron paramagnetic resonance spectroscopic study. *Biochim Biophys Acta* 1661:135–143.
28. Wang R (2004) *Signal Transduction and the Gasotransmitters: NO, CO, and H2S in Biology and Medicine* (Humana Press, Totowa, NJ), p 377.
29. Urban-Ciecko J, Barth AL (2016) Somatostatin-expressing neurons in cortical networks. *Nat Rev Neurosci* 17:401–409.
30. Chachlaki K, Garthwaite J, Prevot V (2017) The gentle art of saying NO: How nitric oxide gets things done in the hypothalamus. *Nat Rev Endocrinol* 13:521–535.
31. Biojone C, Casarotto PC, Joca SR, Castrén E (2015) Interplay between nitric oxide and brain-derived neurotrophic factor in neuronal plasticity. *CNS Neurol Disord Drug Targets* 14:979–987.
32. Zhang J, et al. (2016) Presynaptic excitation via GABAB receptors in habenula cholinergic neurons regulates fear memory expression. *Cell* 166:716–728.
33. Tuesta LM, et al. (2017) GLP-1 acts on habenular avoidance circuits to control nicotine intake. *Nat Neurosci* 20:708–716.
34. Hu F, Ren J, Zhang JE, Zhong W, Luo M (2012) Natriuretic peptides block synaptic transmission by activating phosphodiesterase 2A and reducing presynaptic PKA activity. *Proc Natl Acad Sci USA* 109:17681–17686.
35. Lenn NJ (1976) Synapses in the interpeduncular nucleus: Electron microscopy of normal and habenula lesioned rats. *J Comp Neurol* 166:77–99.
36. Garthwaite J (2008) Concepts of neural nitric oxide-mediated transmission. *Eur J Neurosci* 27:2783–2802.
37. Jayakar SS, et al. (2014) PACAP induces plasticity at autonomic synapses by nAChR-dependent NOS1 activation and AKAP-mediated PKA targeting. *Mol Cell Neurosci* 63: 1–12.
38. Whiteaker P, et al. (2009) Pharmacological and immunochemical characterization of alpha2* nicotinic acetylcholine receptors (nAChRs) in mouse brain. *Acta Pharmacol Sin* 30:795–804.
39. Balestra B, et al. (2000) Chick optic lobe contains a developmentally regulated alpha2alpha5beta2 nicotinic receptor subtype. *Mol Pharmacol* 58:300–311.
40. Lotfipour S, et al. (2013) Targeted deletion of the mouse α2 nicotinic acetylcholine receptor subunit gene (Chrna2) potentiates nicotine-modulated behaviors. *J Neurosci* 33:7728–7741.
41. Berrettini W, et al. (2008) Alpha-5/alpha-3 nicotinic receptor subunit alleles increase risk for heavy smoking. *Mol Psychiatry* 13:368–373.
42. Wang S, et al. (2014) Significant associations of CHRNA2 and CHRNA6 with nicotine dependence in European American and African American populations. *Hum Genet* 133:575–586.
43. Miwa JM, et al. (2006) The prototoxin lynx1 acts on nicotinic acetylcholine receptors to balance neuronal activity and survival in vivo. *Neuron* 51:587–600.